IJAME

Int. J. of Applied Mechanics and Engineering, 2025, vol.30, No.2, pp.31-45
DOI: 10.59441/ijame/200966

ANALYTICAL AND NUMERICAL MODELING OF SHALLOW WATER FLOW IN A CHANNEL: THEORETICAL APPROACHES AND SIMULATIONS

Taofic BACHAROU[1], Daniel SABI TAKOU[*2] and Jamal ADETOLA[3]
[1]Civil Engineering Department, Ecole Polytechnique d'Abomey-Calavi, Université d'Abomey-Calavi, BENIN
[2]Fundamental Sciences Department, Ecole Polytechnique d'Abomey-Calavi, Université d'Abomey-Calavi, BENIN
[3]Mathematical Modelisation Department, Université Nationale des Sciences,Technologie, Ingnierie et Mathéematiques, Abomey, BENIN

E-mail: sabitakoudaniel11@gmail.com

This study focuses on the modeling and simulation of shallow water flows in a channel through the application of the Saint-Venant equations. Two main approaches were explored: an analytical solution and a numerical method based on finite difference discretization. The analytical solution provides exact expressions for water depth and velocity under simplified conditions serving as a benchmark for validating numerical simulations. The numerical method, on the other hand, captures more complex dynamics such as wave propagation and nonlinear interactions between sections of the channel. The simulations reveal an inverse relationship between water depth and flow velocity, confirming the validity of the governing equations. Moreover, the influence of parameters such as channel slope, flow rate, and boundary conditions on the systems dynamics is clearly illustrated. The comparative analysis of the two approaches shows that the finite difference method is a powerful tool for practical applications in hydraulic engineering, allowing for the accurate modeling of real-world phenomena while offering greater flexibility compared to idealized analytical solutions.

Key words: flow modeling, water depth, rectangular channel, Froude number, numerical simulation.

1. Introduction

Modeling shallow water flow is a crucial topic in fluid mechanics, particularly in civil and environmental engineering applications [1-11]. The ability to simulate and predict flow behavior in shallow environments such as rivers, lakes, estuaries and artificial channels is essential for the design and management of water infrastructure, flood forecasting, sediment transport and coastal engineering. Over the past decades, many researchers have contributed to the advancement of analytical and numerical methods applied to shallow water flows. The modeling of shallow water flows flows [1-4] and [5] is based on the Saint-Venant equations, first formulated in the 19th century. These equations describe the conservation of mass and momentum in shallow water systems through a set of hyperbolic partial differential equations. Saint-Venant's pioneering work laid the foundation for future hydrodynamic models, which were refined and adapted for various environmental and engineering applications. For example, R.J. LeVeque [6] explored the use of finite difference methods to solve these equations, highlighting the efficiency and accuracy of these techniques when applied to shallow water systems. LeVeque's work [7] showed that finite difference methods could effectively deal with both steady and transient flow conditions, making them an ideal solution for a wide range of hydrodynamic problems.

Abbott and Basco [8] contributed significantly to the field by studying finite element and finite volume methods, both widely used in the simulation of complex fluid dynamics. Their research highlighted the advantages and limitations of these numerical methods, showing that different approaches may be better suited

[*] To whom correspondence should be addressed

to specific types of flow problems. For instance, finite element methods are often preferred for irregular geometries and complex boundary conditions, while finite difference methods excel in problems where the computational domain is regular and structured.

More recently, García-Navarro *et al.* [9] introduced advanced numerical techniques integrating turbulence modeling, sediment transport, and complex boundary conditions into simulations of shallow water flows. These models have played a crucial role in improving our understanding of shallow water systems under natural and human influences, such as storm surges, dam breaks, and urban flooding. The work of Madsen *et al.* [1] further expanded these capabilities by incorporating adaptive mesh techniques, allowing numerical models to dynamically adjust the resolution of the computational grid, thereby increasing accuracy without significantly raising computational costs.

This report builds on these foundational contributions by developing a robust framework for modeling shallow water flow through both analytical and numerical solutions. Emphasis is placed on solving the governing equations of shallow water flows using finite difference discretization and analytical function representation, providing a comprehensive analysis of flow behavior in a defined channel. This dual approach allows for a more detailed understanding of the physical processes involved and facilitates the comparison of results from different methodologies.

In this paper, we investigate classes of exact solutions for the SW equations [8]. In section *2*, we present the shallow-water model. In section *3*, we use the change of variables transforming the SW model into the ordinary differential equations (ODEs) to obtain the analytical solution. In Section *4*, the proposed numerical method to study the influence of physical parameters. Key results and observations are presented in section *5*. Then follows conclusion in section *6*.

2. Shallow water model

The starting point of our study is the shallow-water (SW) equations governing one-dimensional flow down open channels with transversal rectangular section:

$$\begin{cases} \dfrac{\partial H}{\partial t} + V\dfrac{\partial H}{\partial \xi} + \dfrac{S}{b}\dfrac{\partial V}{\partial \xi} = 0, \\ \dfrac{1}{g}\dfrac{\partial V}{\partial t} + \dfrac{V}{g}\dfrac{\partial V}{\partial \xi} + \dfrac{\partial H}{\partial \xi} = i_o - i_{tp}. \end{cases} \tag{2.1}$$

H, V stand for the variation of water height and fluid velocity above the channel bed respectively; the functions V, H satisfy the initial and boundary conditions

$$H(\xi,t) \vee t = 0 = H(\xi,t)|_{\xi=0} = H_0, \quad V(\xi,t) \vee |_{t=0} = V(\xi,t) \vee |_{\xi=0} = V_0, \qquad H_0; V_0 = const \tag{2.2}$$

$(\xi,t) \in [0,L] \times [0;T]$, L is the channel length.

3. Analytical solutions

In this section we provide analytical solutions to shallow-water equations. We assume the solutions belong to the space of functions that are continuously differentiable with respect to (ξ,t) on $[0,L] \times [0,T]$ i.e. shortly denoted here by:

$$V(\xi,t) \in C^{1,1}_{\xi,t}\left([0,L] \times [0,T]\right), \quad H(\xi,t) \in C^{1,1}_{\xi,t}\left([0,L] \times [0,T]\right). \tag{3.1}$$

Consider the following change $z=-C_w t+\xi$ and $V(z)=V(\xi,t),\quad H(z)=H(\xi,t)$ where C_w is the speed of propagation of the roll waves [5]. Let's state with the following result.

Theorem (3.1).The solutions H, V of the system (2.1) satisfying the conditions (2.2) are defined by the functions

$$V(z)-C_w=(V_0-C_w)e^{\frac{-2b}{s}(H-H_0)}, \tag{3.2}$$

$$H(z)-H_0+\frac{(V_0-C_w)^2}{2g}\left[e^{\frac{2b}{s}(H-H_0)}-1\right]=(i_o-i_{tp})z \tag{3.3}$$

and the fluid flow down the channel can be computed as:

$$Q(\xi,t)=b_0\left(h_0+H(\xi,t)\right)V(\xi,t), \tag{3.4}$$

where H, V are the solutions of the system and $z=\xi-C_w t$ with $-C_w$ the speed of propagation of the roll waves.

Proof (3.1). Let transform the system (2.1) into the linear form: As known $i_{tp}=\frac{Q^2}{K^2}$ where Q value of the fluid flow and K the module of the fluid flow in the section denote by $\Delta H;\Delta V$ the variation of the height and the velocity respectively. From the hydraulic we can write:

$$\left(\frac{K}{K_0}\right)^2=\left(\frac{H_0+\Delta H}{H_0}\right)^x \Leftrightarrow K^2=K_0^2\left(1+\frac{\Delta H}{H_0}\right)^x \tag{3.5}$$

$$\Leftrightarrow K^2\approx K_0^2\left(1+\frac{\Delta H}{H_0}x\right), \tag{3.6}$$

and

$$Q^2=Q_0^2\left(1+\frac{2\Delta V}{V_0}+\frac{2b_0}{S_0}\Delta H\right), \tag{3.7}$$

from (3.6) and (3.7) we obtained

$$i_{tp}=\frac{Q_0^2\left(1+\frac{2\Delta V}{V_0}+\frac{2b}{S_0}\Delta H\right)}{K_0^2\left(1+\frac{\Delta H}{H_0}x\right)}, \tag{3.8}$$

$$\frac{Q_0^2}{K_0^2}\left(1+\frac{2\Delta V}{V_0}+\frac{2b}{S_0}\Delta H\right)\left(1+\frac{\Delta H}{H_0}x\right)^{-1}, \tag{3.9}$$

$$\approx\frac{Q_0^2}{K_0^2}\left(1+\frac{2\Delta V}{V_0}+\frac{2b}{S_0}\Delta H\right)\left(1-\frac{\Delta H}{H_0}x\right), \tag{3.10}$$

$$\approx i_{tp0}\left(1+\frac{2\Delta V}{V_0}+\frac{2b}{S_0}\Delta H-x\frac{\Delta H}{H_0}-2\frac{\Delta V}{V_0}x\frac{\Delta H}{H_0}-\frac{2b}{S_0}\Delta H\frac{\Delta H}{H_0}\right), \tag{3.11}$$

$$\approx i_{tp0}\left(1+\frac{2\Delta V}{V_0}+\frac{2b}{S_0}\Delta H-x\frac{\Delta H}{H_0}\right), \tag{3.12}$$

$$\approx i_{tp0}\left[1+\frac{2\Delta V}{V_0}+\left(\frac{2b}{S_0}-\frac{x}{H_0}\right)\Delta H\right], \tag{3.13}$$

with $i_{tp0}=\dfrac{Q_0^2}{K_0^2}$.

Using this calculation, (2.1) give

$$\frac{1}{g}\frac{\partial V}{\partial t}+\frac{V}{g}\frac{\partial V}{\partial \xi}+\frac{\partial H}{\partial \xi}=i_o-i_{tp0}\left[1+\frac{2\Delta V}{V_0}+\left(\frac{2b}{S_0}-\frac{x}{H_0}\right)\Delta H\right], \tag{3.14}$$

$$i_o\left[1-1-\frac{2\Delta V}{V_0}-\left(\frac{2b}{S_0}-\frac{x}{H_0}\right)\Delta H\right], \tag{3.15}$$

when $i_o=i_{tp0}$, $V=V_0$, $S=S_0$, $b=b_0$,

$$\frac{1}{g}\frac{\partial V}{\partial t}+\frac{V}{g}\frac{\partial V}{\partial \xi}+\frac{\partial H}{\partial \xi}=\frac{-2i_o\Delta V}{V_0}-\frac{2i_o b}{S_0}\Delta H+\frac{xi_o}{H_0}\Delta H, \tag{3.16}$$

$$\frac{1}{g}\frac{\partial V}{\partial t}+\frac{V}{g}\frac{\partial V}{\partial \xi}+\frac{\partial H}{\partial \xi}+\frac{2i_o\Delta V}{V_0}+\frac{2i_o b}{S_0}\Delta H-\frac{xi_o}{H_0}\Delta H=0, \tag{3.17}$$

$$\frac{1}{g}\frac{\partial V}{\partial t}+\frac{V}{g}\frac{\partial V}{\partial \xi}+\frac{\partial H}{\partial \xi}+\left(\frac{2i_o b}{S_0}-\frac{xi_o}{H_0}\right)\Delta H+2i_o\frac{\Delta V}{V_0}=0, \tag{3.18}$$

$$\begin{cases}\dfrac{\partial H}{\partial \xi}+\left(\dfrac{2b}{S_0}-\dfrac{x}{H_0}\right)\Delta H i_o+\dfrac{V}{g}\dfrac{\partial V}{\partial \xi}+2i_o\dfrac{\Delta V}{V_0}+\dfrac{1}{g}\dfrac{\partial V}{\partial t}=0,\\[2ex] V_0 b_0\dfrac{\partial H}{\partial \xi}+b_0\dfrac{\partial H}{\partial t}+S_0\dfrac{\partial V}{\partial \xi}=0.\end{cases} \tag{3.19}$$

In this manner, a system of linear differential equations pertaining to the variation in water height Δh and velocity ΔV is derived. Some coefficients involved in this system (3.19) are morphological parameters of the channel (for example, io), while others can be estimated as a function of a variable. Considering that in many cases, control over the channel's operating regime is achievable solely through water height, let us determine the expression of the coefficients in system (3.19) as a function of H_0: Flow depth in an undisturbed regime. For this purpose, coefficients are concurrently defined for rectangular channels with bottom width B. The

wetted cross-sectional area is denoted as $S_0 = S$, $H_0 = H$. The relationship between the permanent water flow velocity V_0 and the height H_0 can be established based on the condition $i_o = i_{tp}$.

It is known that $i_{tp} = \frac{V_0^2}{C^2 R}$ where C is the Chézy coefficient $\left(m^{1/2}s\right)$; R is the hydraulic radius (m); thus,

$$V_0 = C\sqrt{i_0 R}. \tag{3.20}$$

The Chézy coefficient C is expressed as $C = \frac{1}{n}R^{\frac{1}{6}}$, where n is the coefficient of wall roughness.

The hydraulic radius R for the rectangular channel is expressed as

$$R = \frac{BH_0}{B + 2H_0} = \frac{H_0}{1 + 2\frac{H_0}{B}}. \tag{3.21}$$

By inserting the expression of R into equation (3.20), we obtain for the channel:

$$V_0 = \frac{\sqrt{i_0}}{n} B^{\frac{2}{3}} \left(\frac{\frac{H_0}{B}}{1 + 2\frac{H_0}{B}} \right)^{\frac{2}{3}}. \tag{3.22}$$

Expressing the coefficient *x* in terms of the water height entering the system (3.19), a hydraulic parameter of the wall, regardless of the shape of the wetted cross-section (liquid), as proposed by (V.T Chow, [12]) is given by the formula:

$$x = \frac{2H_0}{3S_0} - \left(5b_0 - 2R\frac{d\gamma}{dH_0} \right), \tag{3.23}$$

where γ represents the wetted perimeter, which is expressed as $\gamma = B + 2H_0$. By incorporating the obtained ratio below into equation (3.23) and applying the requisite derivative, we obtained

$$x = \frac{10B}{2(B + 2H_0)} = \frac{10 + 12\frac{H_0}{B}}{3 + 6\frac{H_0}{B}}. \tag{3.24}$$

Hence, all coefficients of the system of linear Eq.(3.19), which describe gradually varied or steady flow, are directly expressed as functions of H_0. We must now solve this new linear system obtained by introducing the change of variable $z = -C_w t + \xi$ $V(z) = V(\xi, t), H(z) = H(\xi, t)$.

The analytical solution focuses on deriving the water depth (H) and velocity (V) as functions of time and space, based on initial conditions and flow parameters. The derived equations demonstrate the relationship between discharge (Q), water depth (H), and channel slope. The analytical solution is particularly useful for providing exact solutions under simplified conditions, serving as reference points for validating the accuracy of numerical models.

The process begins by linearizing the Saint-Venant equations, assuming small perturbations around a steady-state condition. Using standard techniques such as separation of variables and the method of characteristics, the governing equations are reduced to a set of solvable ordinary differential equations. The final expressions for water depth and velocity are obtained in terms of known parameters, including the channel geometry, slope, and initial flow conditions.

Python-based algorithms are used to compute the analytical solution at discrete time intervals, allowing the visualization of water depth and velocity profiles along the channel. These profiles provide insight into the dynamic behavior of shallow water flows, highlighting the influence of channel geometry, discharge, and external forces on the movement of water.

4. Numerical study of the system

Equations (3.2)-(3.4) express the relationship between the depths of the current in different sections and the distances between these sections and a conventional origin H_0. They establish the connection between the variables $H(\varepsilon,t)$ and $z(\varepsilon,t)$. Equation (3.2) can be transcribed as follows:

$$e^{\frac{-2b}{s}(H-H_0)} = \frac{V(z)-c_w}{V_0-c_w}. \tag{4.1}$$

Using this expression, (3.3) becomes:

$$\left(\frac{V(z)-c_w}{V_0-c_w}\right)^2 - 1 = \left(\frac{u(z)}{u_0}\right)^2 - 1 = \frac{Mu^2(z)}{Mu_0^2} - 1 = \frac{ME_c}{ME_{c(u)}} - 1, \tag{4.2}$$

with $u(z)=V(z)-c_w$: being the velocity at distance $z(\varepsilon,t), u_0 = V_0 - c_w$: the average velocity of the liquid, M: the specific kinetic energy, and $E_{c(u)}$: the kinetic energy for the average velocity.

The kinetic energy of a particle with mass mm moving at velocity $u(z)$ will be $\frac{mu^2}{2}$, and for the entire flow within the given section S, the total energy will be the summation of such kinetic energies:

$$ME_c = \int_s \frac{mu^2}{2} = \int_s \frac{\rho dQu^2}{2} = \int_s \frac{\rho dSu^3}{2}. \tag{4.3}$$

The energy calculated for the average velocity u_0 within the current section

$$ME_{c(u_0)} = \frac{mu_0{}^2}{2} = \frac{\rho dQu_0{}^2}{2} = \frac{\rho dSu_0{}^3}{2}. \tag{4.4}$$

Consequently

$$\frac{ME_c}{ME_{c(u_0)}} = \frac{E_c}{E_{c(u_0)}} = \frac{\int_s \frac{\rho dSu^3}{2}}{\frac{\rho dSu_0{}^3}{2}} = \frac{\int_s u^3 ds}{Su_0^2} = \alpha. \tag{4.5}$$

If we assume that $u = u_0 \pm \Delta u$, after the transformations, we obtain:

$$\alpha = 1 + \frac{3}{S}\int_s \left(\frac{\Delta u}{u_0}\right)^2 ds. \tag{4.6}$$

This implies that $\alpha > 1 \vee E_c > E_c(u_0)$. Equation (4.6) represents the kinetic energy coefficient as follows:

$$e^{\frac{-2b}{s}(H-H_0)} \approx 1 + \frac{3}{S}\int \frac{\Delta u}{u_0} ds \approx \alpha, \tag{4.7}$$

which is the Coriolis coefficient.
So that, considering (3.2), we can transcribe equality (3.3) as follows:

$$H(z) - H_0 = \frac{(V_0 - c_w)^2}{2g}(\alpha - 1) = i_o - i_{tp}, \tag{4.8}$$

$$H(z) - H_0 = \frac{\alpha^* (V_0 - c_w)^2}{2g}(\alpha - 1) = (i_0 - i_{tp}), \tag{4.9}$$

where the coefficient α^* for straight turbulent currents is equal to $0.05 / 0.10$.

In other cases, the value of the coefficient α^* may be significantly larger.
Equations (3.2) and (3.3) provide the analytical solution as well as the initial condition in implicit form.
Solving the implicit equation (3.3) is done by plotting the characteristic curve $z = -c_w * t + \varepsilon$ from the initial conditions u such that:

$$u + e^{-2u} - 1 = 2z. \tag{4.10}$$

For the simulations, a length z equal to $50m$ is taken, and the boundary condition for $z = 0$ is provided.

The solution (Fig.1) depicts the evolution of the free surface from an initial height H_0 to the level $H(z)$, showing that when u is negative and close to 0 , the initial head decreases in favor of kinetic head, which increases with velocity and consequently with z . As u increases, the extent of the water line z decreases abruptly to reach a minimum level $(z_{min} = -0.77$ for $u = 0.34)$ before slowly rising again. Adanhounme and Codo [2] also observed a decrease in water depth with distance under similar inclined flow conditions. They showed that in channels with steeper slopes, the reduction in depth is more pronounced, which is corroborated by our results. However, in Ball's [4] work on paraboloidal geometries, the dynamics are different due to rotational effects, where the observed waves increase with distance in certain configurations, contrary to the decrease observed in our figures.

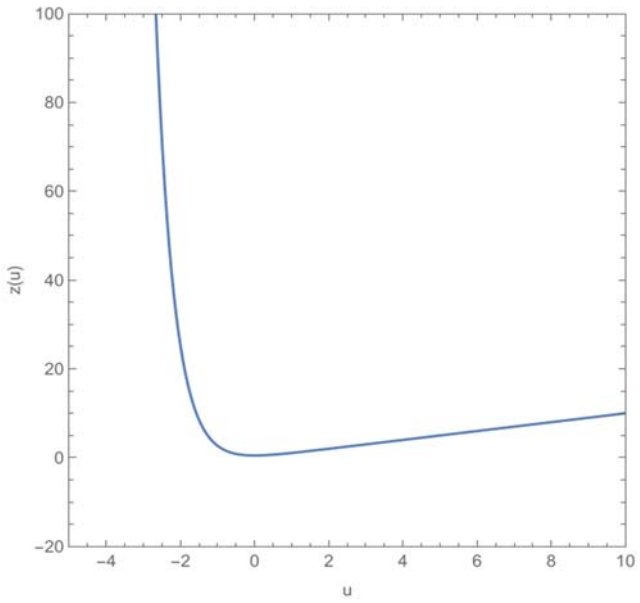

Fig.1. Evolution of the free surface $z(u)$.

The water level (H) represents the flow depth at a given point in the channel at various times (see Fig.2). This depth is influenced by factors such as the channel slope, cross-sectional area, and gravitational forces governing the flow. Based on the presented curves, we observe a gradual variation in H along the channel, with fluctuations corresponding to wave propagation within the channel. This indicates a transient flow influenced by hydraulic conditions such as slope and wall roughness.

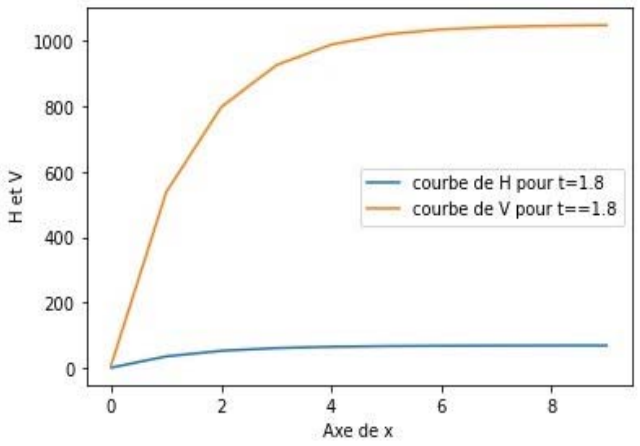

Fig.2. Water level (H) and velocity (V) curves at different times.

The flow velocity (V) corresponds to the amount of water displacement per unit time at various points along the channel. It is governed by the channel's slope, friction losses, and flow depth. The velocity profile evolves over time, indicating transient flow behavior. The evolution of V is associated with friction losses and depth variations. An initial acceleration followed by deceleration suggests that the system is influenced by kinetic energy dissipation through interactions with the channel bed and side walls.

The variations in water level (H) over time reveal a progressive evolution of wave height, typical of transient flow models. These results align with the work of Chow *et al.* [2], which exhibited similar profiles in non-uniform channel flows. The studies by Saint-Venant [13] and Madsen and Sørensen [14], which employed shallow water wave equations, demonstrated that water height in a channel depends on the slope and bed characteristics. The results obtained in the present work are consistent with these studies, especially concerning wave propagation in unsteady systems.

The velocity curve (V) varies over time and distance, influenced by the hydraulic gradient and friction. The velocity reaches an initial peak and then gradually decreases, reflecting transient flow conditions. Madsen and Sørensen [14] observed similar behavior, with a rapid increase in velocity followed by stabilization. The velocity variations in the current model are consistent with their findings, though the maximum velocities observed here are slightly lower, likely due to the relatively low slope (0.1) of the channel used in this study.

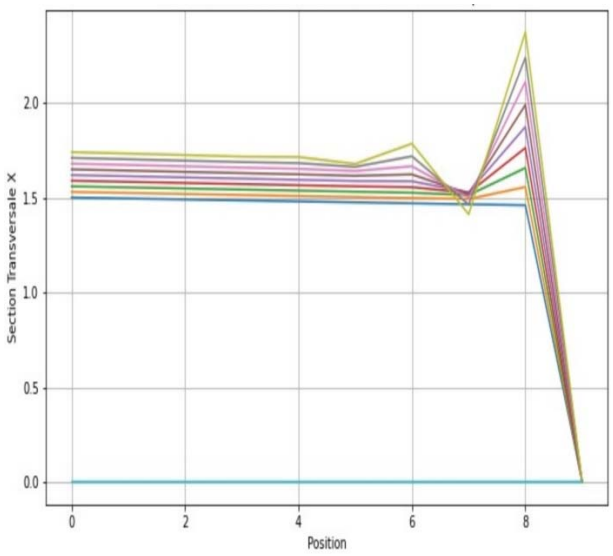

Fig.3. Water level (H) and velocity (V).

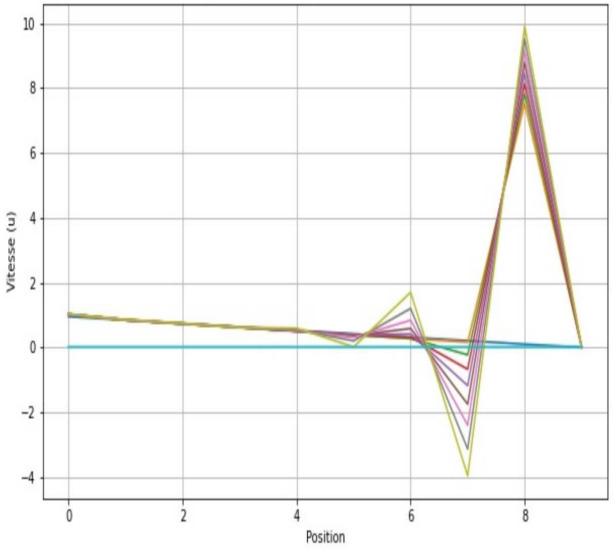

Fig.4. Water level curve (H) curves at different times.

This Fig.3 shows the water level at a given time along the length of the channel. The results depict a profile following an oscillating trend, where the water rises and falls due to wave propagation and frictional forces. The works of Chow [12] and Dingman [15] on open-channel flow have demonstrated that water level variations are strongly influenced by the channel's cross-sectional geometry and the initial flow conditions. In the present study, the channel depth and friction similarly affect water level fluctuations, aligning with their findings. If the channel slope or friction were higher, as noted in some of Hervouet's [16] studies on numerical flow modeling, we might observe more pronounced peaks in the water level.

Figure 4 shows that velocity varies along the channel's length. The velocity decreases at certain points, indicating a transition between faster and slower flow regimes, influenced by depth and frictional losses. The works of Saint-Venant and the numerical simulations of LeVeque [17] also demonstrate a gradual decrease in velocity as waves propagate through the channel, particularly in cases with a low slope, as seen in the present simulation. The results align with these observations, although a steeper slope in some cases would have produced higher velocities.

The studies by Bellos and Salingaros [18], which examined flows in high-slope channels, reported higher velocities and faster transitions in velocity variation. The results obtained in this work, with a moderate slope of 0.1 are more suited to low-slope channels, which explains the lower velocities observed. Referring to critical parameters, the main variables influencing the results are the channel slope (0.1), the initial water

level (*1.5 m*), and the friction coefficient (equal to *0.03*). These values correspond to typical hydraulic studies on shallow channels, but variations in these parameters would have led to different results, particularly in the observed maximum velocities.

In summary, the results are generally consistent with previous studies. The Saint-Venant equations and modern numerical models (Chow [12], Madsen and Sørensen [14]) confirm that the water level and velocity profiles follow expected trends. The moderate slope and frictional losses temper the observed velocities, unlike studies with steeper slopes or smoother channels.

In order to analyze the problem, we choose to non-dimensionalize Eqs (3.2) and (3.3).

Referring to basic concepts of hydraulics, we have: $s = bH$ and $\frac{b}{s} = \frac{1}{H}$, then

$$\frac{b}{s}(H - H_0) = \frac{1}{H}(H - H_0) = \frac{H_0}{H}\left(\frac{H}{H_0} - 1\right). \tag{4.1}$$

By the following variable reset:

$$h = \frac{H}{H_0}, V_0 = \sqrt{2gH_0}, \quad F_r = \frac{V_g}{\sqrt{gH_0}}, \quad v = \frac{V}{V_0}, \tag{4.12}$$

we obtained

$$(4) \Rightarrow \frac{V(z)}{V_0} - \frac{c_w}{V_0} = \left(1 - \frac{c_w}{V_0}\right) e^{\frac{-h-1}{h}}. \tag{4.13}$$

Also,

$$c_w = \sqrt{gH_0} \Rightarrow \frac{c_w}{V_0} = \frac{1}{F_r}, \tag{4.14}$$

$$(39) \Rightarrow v(z) = \frac{1}{F_r} + \left(1 - \frac{1}{F_r}\right) e^{\frac{-h-1}{h}}, \tag{4.15}$$

$$(5) \Rightarrow \frac{H(z)}{H_0} - 1 + \frac{(V_0 - c_w)^2}{2gH_0}\left(e^{-2\frac{H}{H_0}\left(\frac{H}{H_0}-1\right)} - 1\right) = (i_o - i_{tp})\frac{z}{H_0}. \tag{4.16}$$

So that,
$$h - 1 + \frac{1}{2}(F_r - 1)^2\left(e^{-2\left(\frac{h-1}{h}\right)} - 1\right) = (i_o - i_{tp})\frac{z}{H_0} \tag{4.17}$$

hence
$$(i_o - i_{tp}) = \frac{H_0}{z}\left[h - 1 + \frac{1}{2}(F_r - 1)^2\left(e^{-2\left(\frac{h-1}{h}\right)} - 1\right)\right]. \tag{4.18}$$

This expression leads, after some calculations, to:

$$i_{tp} = i_o\left(1+\frac{2\Delta V}{V_0}+\left(\frac{2b_0}{S_0}-\frac{x}{H_0}\right)\Delta H\right) = i_o\left(1+\frac{2(V-V_0)}{V_0}+(2-x)\left(\frac{H}{H_0}-1\right)\right). \tag{4.19}$$

We get the difference

$$i_{tp} - i_o = i_o\left(2(v-1)+(h-1)(2-x)\right), \tag{4.20}$$

(4.18) and (4.19) lead,

$$h-1+\frac{1}{2}(F_r-1)^2\left(e^{-2\left(\frac{h-1}{h}\right)}-1\right) = -i_o\left(2(v-1)+(h-1)(2-x)\right)\frac{z}{H_0} \tag{4.21}$$

and (4.20) in (4.21) lead

$$\begin{aligned} &h-1+\frac{1}{2}(F_r-1)^2\,e^{-2\left(\frac{h-1}{h}\right)}-\frac{1}{2}(F_r-1)^2 = \\ &= 2i_o\frac{(F_r-1)}{F_r}\left(e^{-2\left(\frac{h-1}{h}\right)}-1\right)\frac{z}{H_0}+i_o(h-1)(2-x)\frac{z}{H_0}. \end{aligned} \tag{4.22}$$

Equation (4.22) represents an implicit function $h(z) = h(-c_w * t + \varepsilon)$, parametrized by $F_r, \frac{H_0}{b}$ and i_0.

Let's examine the variations of h with respect to z for different parameter values.

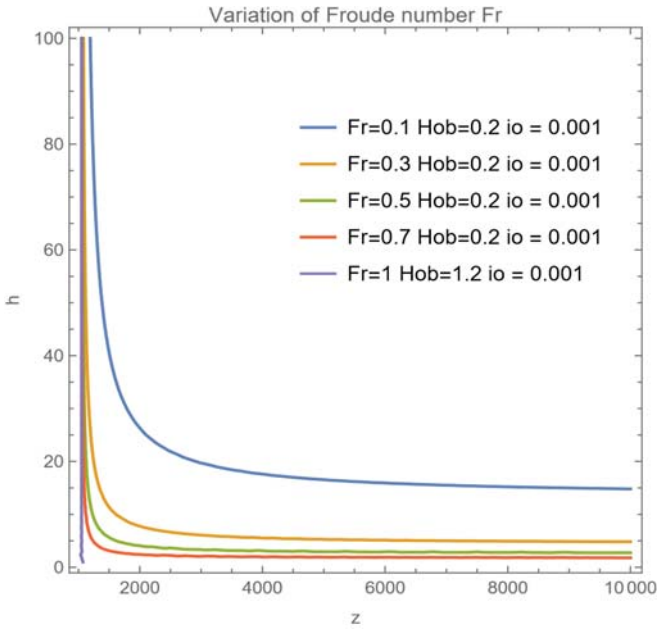

Fig.5. Influence of the Froude number F_r on the flow height.

The variation of the Froude number leading to a regime change imposes a torrential regime at the inlet and a fluvial regime at the outlet. The function defining the water height undergoes a regime change via a hydraulic jump halfway through the transition zone (Fig.5). Additionally, it is observed that the height decreases with increasing z and depends on the value of the initial height. For the same water height value $(H = constant)$, z increases with increasing H_0, and z grows more rapidly when H_0 is high.

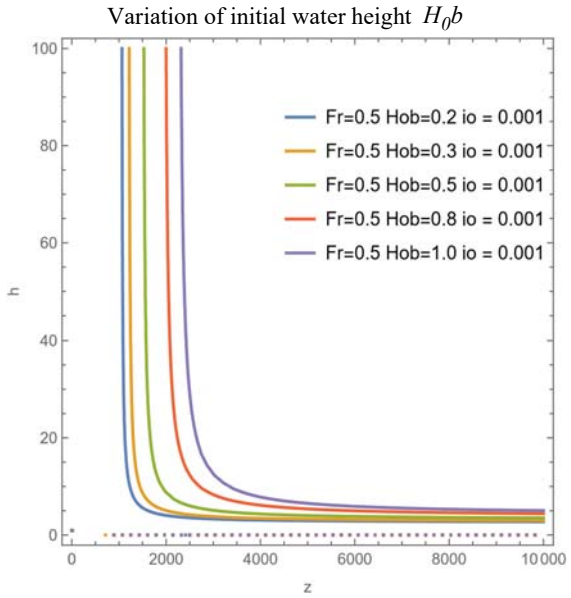

Fig.6. Influence of the variation of initial water height H_0b.

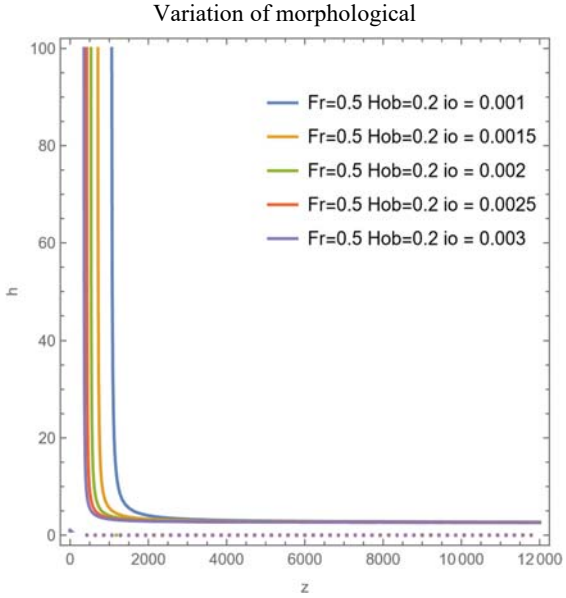

Fig.7. Influence of morphological parameters i_0 on the flow height.

Figure 6 shows that changes of the initial water height H_0b affect the flow height h. The flow height decreases rapidly as z increases, then stabilizes at a constant value.
The value of H, a function of z, decreases more rapidly with a steeper slope than with a gentler slope, which results in a more extended z (Fig.7).
The initial slope i_0 (Fig.7) significantly affects the flow height, with steeper slopes generally leading to faster, shallower flows, while flatter slopes can result in slower, deeper flows.

Analytically, the relationship is governed by fundamental principles of fluid mechanics, influenced by both gravitational forces and frictional resistance from the channel or surface. Between $z = 500$ and $z = 1500$ (Fig.7), the value of h decreases rapidly and tends toward a limit height of $h_{\text{lim.}} = 5$, regardless of the value of the morphological parameter i_0. From $z = 1500$ to infinity value, h remains unchanged and retains this limit value. These observations indicate that neither the morphological parameter i_0 nor z influence the flow height h. The fluid flow velocity depends on the Froude number F_r. An increase in the value of F_r leads to a decrease in velocity, in line with theoretical values reported in the literature (Fig.8). It is also noted that an increase in flow height h does not affect the fluid velocity. Although the analytical solution provides valuable insights, it is often limited to idealized scenarios. For real-world applications, more complex and accurate models are required. For this purpose, a finite difference discretization of the shallow water flow equations has been developed. The finite difference method was chosen for its simplicity and efficiency in solving hyperbolic partial differential equations on structured grids.

The discretization process begins by dividing the computational domain (the channel) into a series of discrete points or grid cells. The governing equations are then approximated at each grid point using finite differences for the temporal and spatial derivatives. Specifically, a forward difference is applied for time integration, and a centered difference is used for spatial derivatives, ensuring second-order accuracy in space.

The Python code developed for this method iterates at each time step, updating the water depth and velocity at each grid point based on the current state of the system. Boundary conditions are carefully handled to ensure that the physical constraints of the system (such as no-flow boundaries at the channel edges) are respected. The results are visualized as time dependent water depth and velocity profiles, which can be compared to the analytical solution to evaluate the accuracy of the numerical model.

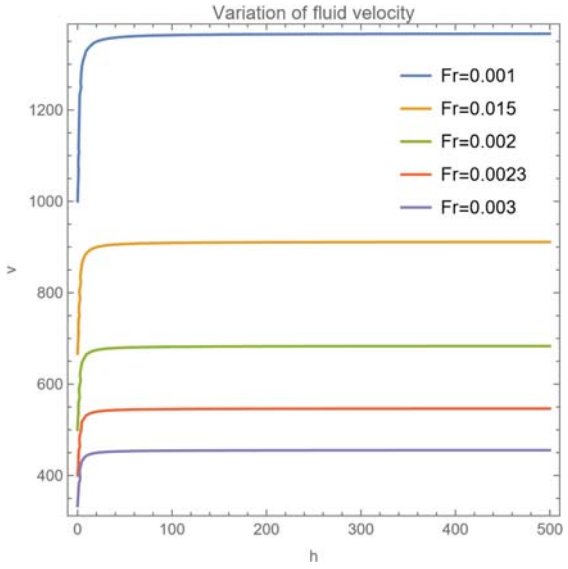

Fig.8. Variation of fluid velocity.

5. Key results and observations

Analytical and numerical models provide complementary insights into the behavior of shallow water flow in a channel. The analytical solution confirms the expected behavior of the system under idealized conditions, while the numerical model is capable of capturing more complex dynamics, such as the evolution of flow patterns over time and the impact of nonlinear effects. Numerical simulations reveal several important trends:

As expected, an increase in flow rate results in a proportional rise in water depth, as governed by the continuity equation. However, the numerical model captures additional details, such as wave development and interactions between different sections of the channel.

The flow velocity increases with the channel slope and decreases as water depth increases. This inverse relationship between water depth and velocity is consistent with the conservation of momentum and is accurately captured by both models.

The numerical model also captures wave propagation along the channel, which is not easily predicted by the analytical solution. This highlights the importance of numerical methods in studying real fluid dynamics, where nonlinear effects and external forces play a major role.

6. Conclusion

The comparative analysis between analytical and numerical solutions for shallow water flow highlights the strengths and limitations of each approach. The analytical solution offers an exact representation of flow

under idealized conditions, serving as a benchmark for numerical validation. However, it is constrained by assumptions of linearity and simplicity, limiting its applicability to real-world problems.

On the other hand, the numerical model based on finite differences offers a more flexible and powerful framework for simulating complex flow dynamics. It is capable of handling nonlinear effects, such as wave propagation and interactions between different sections of the flow, which are not easily captured by the analytical solution. Python-based simulations provide accurate and efficient solutions for real-time and large-scale applications, making the numerical model a valuable tool for engineers and hydrologists.

The results obtained in this study confirm that shallow water flow can be effectively modeled by combining analytical and numerical methods. The finite difference method, in particular, proves to be a robust and efficient tool for simulating shallow water dynamics in channels. The accuracy of the numerical model is validated by comparison with the analytical solution, and the results align with the expected physical behavior of the system.

In conclusion, this study contributes to the ongoing development of shallow water flow modeling techniques by providing both theoretical insights and practical tools for simulation. Future work could focus on extending the model to include additional factors such as sediment transport, turbulence, and multidimensional flow fields. These improvements would further enhance the accuracy and applicability of the model, making it a valuable resource for both academic research and practical engineering applications.

Future studies could incorporate sediment transport, turbulence, and multidimensional flow fields to improve the model's accuracy and applicability.

Acknowledgements

We would like to express our sincere thanks to the referees for their valuable feedback and constructive comments, which have greatly contributed to improving the quality of this manuscript.

Nomenclature

c_w – the speed of propagation of the roll waves
H – stand for the variation
L – is the channel length
v – water height and fluid velocity
x – is the hydraulic exponent
α – for straight turbulent currents
α^* – straight turbulent currents
γ – represents the wetted perimeter
ε – is spacial variable
ρ – fluid density
ρ_o – being the constant pressure on the free surface

References

[1] Chesnokov A.A. (2009): *Symmetries and exact solutions of the rotating shallow- water equations*.– Euro. J. of App. Math., vol.20, No.5, pp.461-477, https://doi.org/10.1017/S0956792509990064.
[2] Adanhounme V. and Codo F.P. (2012): *Shallow water flow down an inclined open channel: analytical solutions of governing equations*.– International Journal Scientific and Engineering Research, vol.3, No.6, p.1-5.
[3] Ball F.K. (1963): *Some general theorems concerning the finite motion of a shallow rotating liquid lying on a paraboloid*.– J. Fluid Mech, vol.17.pp.240-256, https://doi.org/10.1017/S0022112063001270.
[4] Ball F.K. (1965): *The effect of rotation on the simpler modes of motion of a liquid in an elliptic paraboloid*.– J. Fluid Mech., pp.529-545, https://doi.org/10.1017/S0022112065000952.
[5] Bila N., Mansfield E. and Clarkson P. (2006): *Symmetry group analysis of the shallow water and semi-geostrophic equations*.– Quart. J. Mech. Appl. Math., pp.95-123, DOI:10.1093/qjmam/hbi033.

[6] LeVeque R.J. (1998): *Gradients in high-resolution Godunov methods*.– Journal of Computational Physics, vol.141, pp.541-549, https://doi.org/10.1006/jcph.1998.6058.
[7] LeVeque R.J. (2007): *Finite difference methods for ordinary and partial differential equations: steady-state and time-dependent problems*.– Society for Industrial and Applied Mathematics, vol.33, pp.627-665. DOI:10.1137/1.9780898717839.
[8] Abbott M.B. and Basco D.R. (1989): *Computational fluid dynamics*.– J. Fluid Mech. vol.229, pp.689 https://doi.org/10.1017/S0022112091213233.
[9] García-Navarro P. and Vázquez-Cendón M.E. (2000): *On numerical treatment of the source terms in the shallow water equations*.– Computers & Fluids, vol.29, pp.951-979, https://doi.org/10.1016/S0045-7930(99)00038-9.
[10] Marche F., Bonneton P., Fabrie P. and Seguin N. (2007): *Evaluation of well-balanced bore capturing schemes for 2D wetting and drying processes*.– Int. J. Numer. Methods Fluids, vol.53. pp.867-894, https://doi.org/10.1002/fld.1311.
[11] Brook B.S., Falle S.A. and Pedley T.J. (1999): *Numerical solutions for unsteady gravity driven flows in collapsible tubes: evolution and roll-wave instability of a steady state*.– J. Fluid Mech., vol.396. pp.223-256, https://doi.org/10.1017/s0022112099006084.
[12] Chow V.T. (1959): *Open Channel Hydraulics*.– McGraw-Hill, New York.
[13] Saint-Venant A.J.C. (1871): *Théorie du mouvement non permanent des eaux, avec application aux crues des rivières et a l'introduction de marées dans leurs lits*.– Comptes Rendus des Séances de Académie des Sciences, vol.73, pp.147- 237.
[14] Madsen P.A. and Sørensen O.R. (1992): *A new form of the Boussinesq equations with improved linear dispersion characteristics*. *Part 2. A slowly-varying bathymetry*.– Coastal Engineering, vol.18, No.3-4, pp.183-204, https://doi.org/10.1016/03783839(92)90019-Q.
[15] Dingman S.L. (2002): *Physical Hydrology*.– 2nd Edition, Prentice Hall, Upper Saddle River, p.646.
[16] Hervouet V. (2007): *La mobilité du quotidien dans les espaces périurbains, une grande diversité de modèles de déplacements*.– Norois, vol.205, pp.37-52.
[17] LeVeque R.J. (2002): *Finite Volume Methods for Hyperbolic Problems*.– Cambridge University Press, Cambridge, pp.64-86, doi.org/10.1017/CBO9780511791253
[18] Salingaros N. (1981): *Realization, extension, and classification of certain physically important groups and algebras*.– Journal of Mathematical Physics, vol.22, pp.226-232, doi.org/10.1063/1.524893.

Received: October 27, 2024
Revised: February 7, 2025